THE ELECTRICAL CHARACTERISTICS OF FIXED CHARGE MEMBRANES: SOLUTION OF THE FIELD EQUATIONS

H. G. L. COSTER, E. P. GEORGE, *and* R. SIMONS

From the School of Physics, University of New South Wales, Sydney, Australia

ABSTRACT A theoretical analysis is made of the electrical characteristics of a membrane containing two fixed charge regions, of opposite sign, in contact. Profiles of ion concentrations, electrostatic potential, space charge density, as well as the voltage-current characteristics were obtained by numerical integration of the field equations on a computer. Comparison with the predictions of an earlier analysis of this system (Coster, 1965) shows that the latter is valid to a good approximation for membranes > 70 A in thickness. In particular the form of the electrical characteristics, including the punch-through effect, have been verified by the computer analysis. The range of useful validity of the earlier analysis, the use of Boltzmann statistics when currents are present, and variation of membrane capacitance with applied potential, are discussed in the light of the results obtained.

INTRODUCTION

The electrical properties of fixed charge membranes have long been a subject of interest as a possible model for the cell membrane (e.g., see Meyers and Sievers, 1936 and Teorell, 1953).

The ion exchange properties of these membranes have also been investigated in some detail (Eisenman, 1960, 1962). The potentials developed across such membranes and the ionic fluxes which exist in these systems have recently been analyzed by Karreman and Eisenman (1962) and Conti and Eisenman (1965 *a*, 1965 *b*).

One particular type of fixed charge membrane that has attracted some attention as a likely model for the cell membrane consists of two fixed charge regions, of opposite sign, in contact. Mauro (1962) showed that at the junction of two such lattices space charge regions exist and that such a junction displays the conservative property of capacitance.

Coster (1965) has analyzed the voltage-current characteristics of such a membrane and showed that this system displays rectification. This analysis further predicted that at very large reverse (i.e., hyperpolarizing) potentials the differential resistance decreases again and finally approaches zero at a particular membrane potential. This

rapid decrease in the slope resistance which was referred to as the "punch-through" effect has also been observed experimentally in the membranes of *Characean* cells (Coster, 1965; Coster and Hope, 1968; Williams and Bradley, 1968; Coster, 1969).

In the analysis of Coster a number of simplifying assumptions were made to enable a semianalytic (SA) approach to be used. It was shown by George and Simons (1966) that for very thin membranes, < 50 A, some of these assumptions break down.

In view of the possible relevance of this type of membrane model to biological systems, a more thorough numerical analysis has now been made of this problem, with particular reference to the effect of membrane thickness. The present work was particularly aimed at determining the range of validity of the semianalytic approach and to provide exact solutions for a number of specific cases.

The general form of the results may also be relevant to other membrane models where theoretical calculations, strictly applicable only to thick membranes in equilibrium, are applied to very thin membranes in a steady state.

THEORY AND METHODS

The membrane model to be considered in this paper is depicted in Fig. 1. It is assumed that the fixed charges are homogeneously distributed and are fixed to a lattice which does not contribute to the electrical properties other than in a possible effect on the ion mobility and the macroscopic dielectric constant.

The current density of mobile ions, which move in the solution that permeates the lattice, is given by the following equations:

$$J_p = -kT\mu_p \frac{dP}{dx} - Pq\mu_P \frac{d\psi}{dx}$$

$$J_n = +kT\mu_N \frac{dN}{dx} - Nq\mu_P \frac{d\psi}{dx} \tag{1}$$

where P and N refer to the concentration of positive and negative mobile ions respectively, k is the Boltzmann constant, T the temperature in ^0K, μ_P and μ_n the ion mobilities, ψ the electrostatic potential, and q is the absolute value of the electronic charge. All ions are assumed to be univalent.

The current is taken as positive (depolarizing) when the solution phase in contact with the negative fixed charge region of the membrane becomes positive with respect to the solution phase on the other side.

The variables P, N, and ψ are functions of x, the coordinate normal to the membrane, and are related through the Poisson equation:

$$\frac{d^2\psi}{dx^2} = \frac{-\rho(x)}{\epsilon} \tag{2}$$

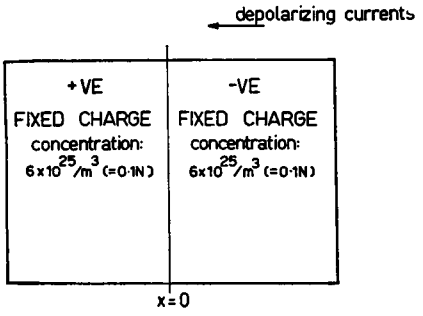

FIGURE 1 Double-fixed charge membrane, in which the region to the left of $x = 0$ contains fixed positive charges, and is in contact with a region containing fixed negative charges to the right of $x = 0$. For the present investigations the fixed charge concentration, F, was taken as 6×10^{25} charges m^{-3} (i.e., 0.1 N). The external solution was taken as 1 mN (i.e., 6×10^{26} m^{-3}). In the external solution the ion mobility was taken as $\mu_0 = 7.6 \times 10^{-8}$ $m^2 s^{-1} v^{-1}$ (appropriate for a 1 mN KCl solution) and the dielectric constant was taken as $\epsilon = 80$. In the membrane the ion mobility was taken as 10^{-3} μ_0 (see text) and the dielectric constant was put equal to 10. The direction of positive (depolarizing) current is indicated on the diagram.

where $\rho(x)$ is the space, or net, charge density, i.e., $\rho = P - N \pm F$ where F is the fixed charge density. ϵ is the dielectric constant (i.e., $\epsilon = \epsilon_r \epsilon_0$; ϵ_r is the relative permittivity and ϵ_0 the permittivity of free space).

In general, equations 1 and 2, cannot be integrated directly for the fixed charge membrane system.

In the semianalytic analysis the following assumptions were made which allowed the electrical characteristics to be determined.

1. When no current flows through the membrane, the mobile ion concentrations satisfy the Maxwell-Boltzmann distribution function.
i.e.,

$$P(x) = P_0 \exp - q[\psi(x) - \psi(-\infty)]/kT$$

and

$$N(x) = N_0 \exp + q[\psi(x) - \psi(-\infty)]/kT \tag{3}$$

where P_0 and N_0 are the concentrations of cations and anions respectively at an infinite distance from the membrane, where the electrostatic potential $\psi(-\infty) = 0$ and $P_0 = N_0$.

2. In moving from the solution phase into the membrane the profiles of electrostatic potential and ion concentrations reach steady levels in distances small compared to the width of each lattice.

The junction of a fixed positive charge region with a fixed negative charge region gives rise to a transition region which is almost completely depleted of mobile ions and where subsequently the space charge density is high (Mauro, 1962). A large junction potential exists across this depletion layer. Furthermore, because of the

much higher total concentration of ions in other regions of the membrane, any applied bias will appear almost completely across this region.

The regions outside the depletion layer in the fixed charge lattices are consequently regions of low field strength and the current densities can be obtained from equations 1 by neglecting the term in the field strength $-d\psi/dx$.

In order to obtain the concentration gradients in this region, the following two additional assumptions had to be made.

3. When a current flows, the concentrations of the ions at the boundary of the depletion layer in one lattice are still related to the corresponding concentrations of these ions at the depletion layer boundary in the other lattice, through the Boltzmann distribution law with the new value for the electrostatic potential across the junction.

4. The changes in the ratio of the majority ions in one lattice to the corresponding minority ions in the opposite lattice when a bias is applied, is taken up by changes in the minority ions rather than the majority ions. This was justified on the grounds that this minimizes the space charge density (and hence energy) in the system.

By idealizing the expected profiles of ψ, ρ, P, and N, i.e., by introducing step changes in place of steeply rising profiles (see Figs. 2 and 3 of Coster, 1965), it was then possible to obtain the dependence of the depletion layer thickness on the applied potential and hence, the complete voltage-current characteristics. The increase in depletion layer thickness when the membrane is hyperpolarized is responsible for the punch-through effect.

Coster's 1965 paper was predominantly concerned with the voltage-current characteristics of the membranes. Since these are determined by the profiles of ion concentration and potential outside the depletion layer, the corresponding profiles inside the depletion layer were not discussed. However, a simple extension of the method described (e.g., by integration of equations 3′ in Appendix B of that paper) enables the complete profiles to be obtained.

For the present studies, numerical computer solutions of the field equations were obtained by the method of George and Simons (1966). For completeness the essential features of this method are here reviewed.

The fundamental difficulty encountered in numerical integration of the field equations is that the boundary conditions are only specified at $x = \pm\infty$. Thus, for $x \to \infty$

$$\frac{dP}{dx} \to 0$$

and

$$J_P = P_1 q \mu_P E_1$$
$$J_n = N_1 q \mu_n E_1 \qquad (4)$$

where E_1 is a constant field strength in the solution phase at large distances from the membrane and P_1 and N_1 are the corresponding concentration of ions.

It was demonstrated by George and Simons that for distances from the fixed charge lattice which are large compared with the Debye length[1], L_D, say at $x = -L$ with $L \gg L_D$

$$E = E_1 + e_1 \exp(\alpha x)$$
$$P = P_1 + p_1 \exp(\alpha x)$$
$$N = N_1 + n_1 \exp(\alpha x) \tag{5}$$

[1] The Debye length, L_D is given by: $L_D = (\epsilon_R \epsilon_0 kT/2q^2P_1)^{1/2}$.

where the second term on the right hand side of each of equations 5, is a small perturbation on the first term. The attenuation constant α is given by

$$\alpha = [(2q^2P_1/\epsilon_R\epsilon_0 kT) + (qE_1/kT)^2]^{1/2}. \tag{6}$$

Of the three constants n_1, p_1, e_1 only one is independent. Taking n_1 as the independent constant the remaining ones are given by (see George and Simons, 1966)

$$e_1 = -n_1[(qE_1 + \alpha kT)/qP_1]$$
$$p_1 = -n_1[(qE_1 + \alpha kT)/(qE_1 - \alpha kT)]. \tag{7}$$

For the computer calculation the current density is specified

$$J = J_P + J_n = P_1 qE_1(\mu_P + \mu_n). \tag{8}$$

For simplicity it was assumed that $\mu_P = \mu_n = \mu$.

An arbitrary value for the constant n_1 in equation 5 is now chosen. Starting at $x = -L$, the field equations were then numerically integrated using a Runga-Kutta routine on an IBM 360/50 computer. The initial conditions at this point being obtained from equation 5, viz.

$$E(-L) = E_1 + e_1 \exp(-\alpha L)$$
$$P(-L) = P_1 + p_1 \exp(-\alpha L)$$
$$N(-L) = N_1 + n_1 \exp(-\alpha L). \tag{9}$$

For the present work a value of $P_1 = N_1 = 6 \times 10^{23}/\text{m}^3$ was used (i.e., 1.0 mN).

The value for n_1 so far is completely arbitrary. n_1 was determined as follows. From symmetry it is evident that at the junction of the positive and negative fixed charge lattices the concentration of negative and positive mobile ions must be equal if the concentrations of these ions in the bulk solution outside the membrane, are equal.

The computer program then adjusted the value of n_1 until at the lattice junction

$$|P - N|/P < 10^{-3}.$$

The number of integrating runs required to achieve this was dependent on the thickness of the membrane and the current density.

Profiles of the electrostatic potential mobile ion concentration, space charge density and current densities were also calculated using the approximate analytical method of Coster (1965).

The above parameters were determined over a wide range of current densities and for membranes 50–200 A in thickness using both methods of analysis. In each case the mobility of the ions in the external electrolyte was taken as $\mu_0 = 7.6 \times 10^{-8} m^2 S^{-1} V^{-1}$. The mobility inside the membrane, μ_i was taken as 10^{-3} μ_0, i.e., $\mu_i = 7.6 \times 10^{-11} m^2 S^{-1} V^{-1}$ as this value had been shown by George and Simons to be the one which gave voltage-current characteristics similar to those observed for some cellular membranes.

RESULTS

Voltage-Current Characteristics

The voltage-current characteristics for membranes of 50, 70, 100, and 200 A total width are shown in Fig. 2. The full curves were obtained from the semianalytic (SA) analysis of Coster while the points were obtained from the computer analysis.

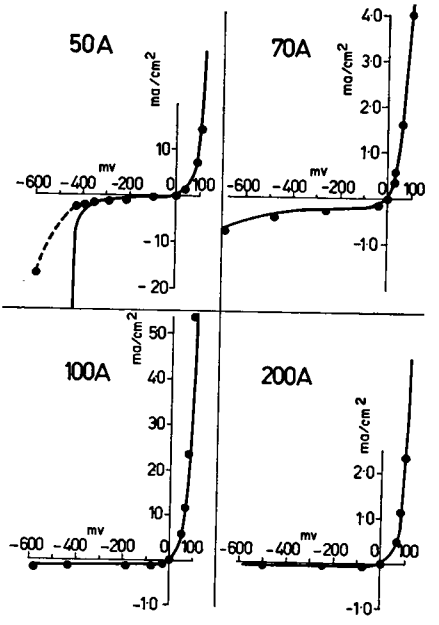

FIGURE 2 The voltage-current characteristics for double-fixed charge membranes of 50, 70, 100, and 200 A total thickness. The full curves were obtained from the semianalytic analysis while the points marked were obtained from the computer analysis. Note that the current scale in the case of the 50 A membrane is different from the others.

It can be seen that the two approaches are in almost perfect agreement over the range of currents shown, the major exception to this being at large hyperpolarizing currents in the 50 A membrane as punch-through is approached. This latter effect, which was predicted by the semianalytic analysis, is clearly verified for this membrane although the computer analysis shows that the potential at which the slope conductance rapidly increases is more negative (~100 mv) than the predicted value. Limitations on computer accuracy prevented attainment of results near the punch-through region for thicker membranes.

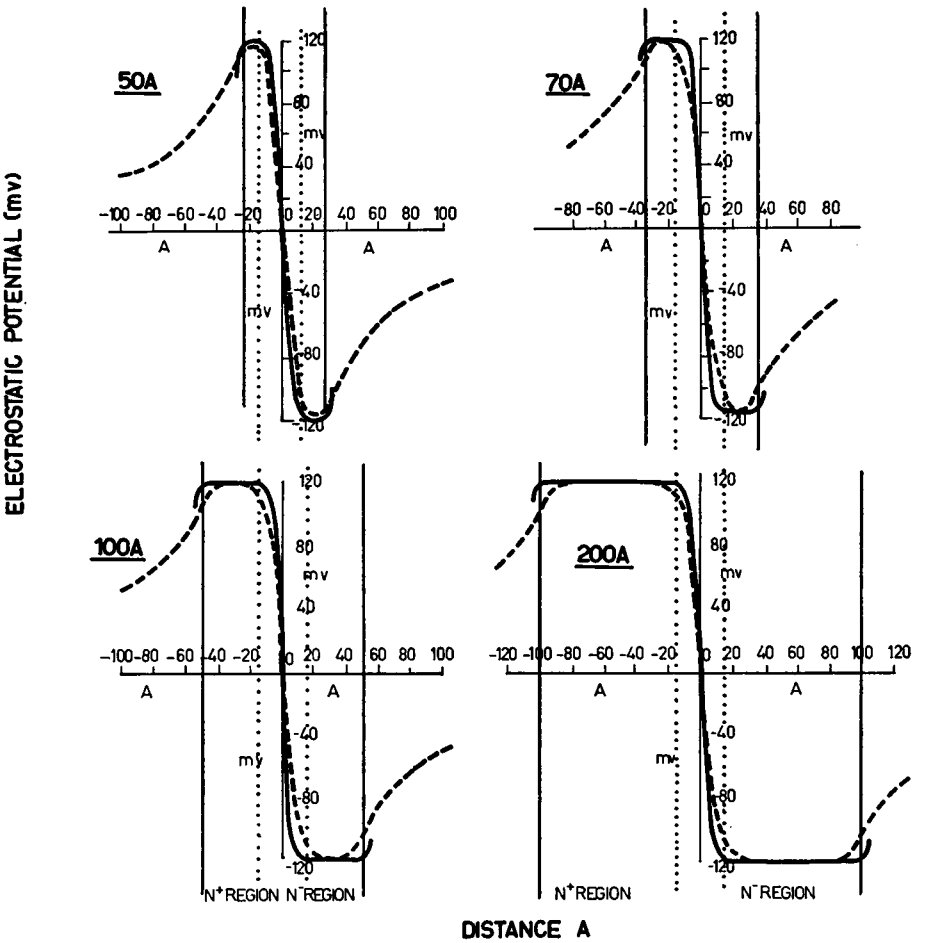

FIGURE 3 Profiles of electrostatic potential for a 50, 70, 100, and 200 A double fixed charge lattice at zero current density. In each case the full curves were obtained from the semianalytic analysis while the broken curves represent the results of the computer solutions. The depletion layer boundary, as calculated from the semianalytic approach, is indicated by the dotted vertical lines.

The Potential Distribution

The profiles of electrostatic potential for a 50, 70, 100, and 200 A membrane at zero current density are shown in Fig. 3. The full curves were derived from the semianalytic treatment, whereas the broken curves were obtained from the computer analysis. The depletion layer region as defined by the SA model is also indicated.

The agreement between the two sets of results is generally fairly good and improves with increasing membrane thickness.

It can be seen that there are regions in the membrane, outside the depletion layer (indicated by dotted vertical lines), where the electrostatic field strength, $-d\psi/dx$, equals zero. In the SA (semianalytic) approach it was assumed that $-d\psi/dx$ is small everywhere outside the depletion layer. It is apparent from Fig. 3 that the validity of this assumption improves with increasing membrane width.

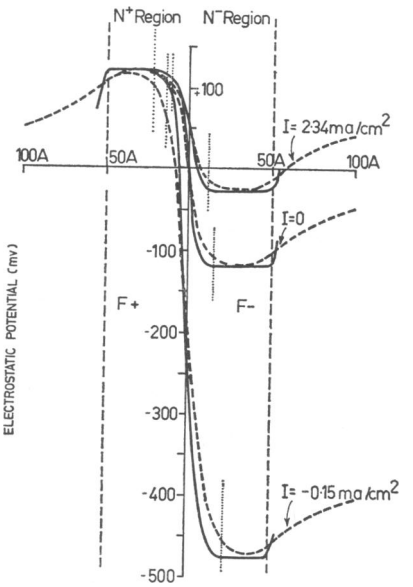

FIGURE 4 The profiles of electrostatic potential for a 100 A membrane at a current density J = 2.34 ma/cm² (depolarizing), J = 0 and J = −0.15 ma/cm² (hyperpolarizing). The full curves were obtained from the semianalytic analysis and the broken curves from the computer results. The depletion layer boundary in each lattice, for each current density, is indicated by the dotted vertical lines.

One of the fundamental assumptions made in the semianalytic approach was that all the applied bias appears across the depletion layer. The potential profile at three current densities for a 100 A membrane is shown in Fig. 4. The full curves were obtained from the SA model and the broken curves from the computer results. It is evident from this figure that virtually all of the additional potential appears across the depletion layer.

The Depletion Layer and the Punch-Through Effect

In the semianalytic analysis it was assumed that in the depletion layer the fixed charges are almost completely uncompensated by the mobile counterions and thus

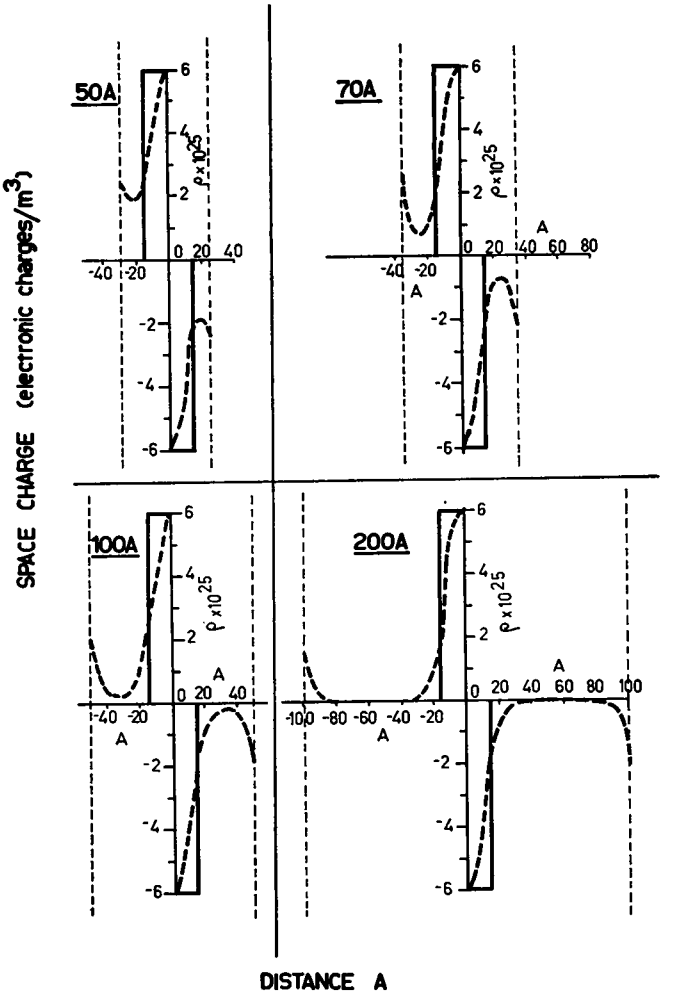

FIGURE 5 Profiles of space charge density for a 50, 70, 100, and 200 A double fixed charge membrane at zero current density. The full curves are the idealized profiles assumed in the semianalytic model while the dashed curves were obtained from the computer analysis.

set up a strong space charge region. In the fixed charge lattices outside the depletion layer it was further assumed that the counterions almost completely neutralize the fixed charge—i.e., a negligible space charge exists in these regions. With these assumptions the depletion layer width could then be calculated (see Appendix B in Coster, 1965).

From the computer results the space charge density distribution was obtained as a function of membrane thickness and current density. The results for the 50, 70, 100, and 200 A membranes at zero current density are shown in Fig. 5. The idealized

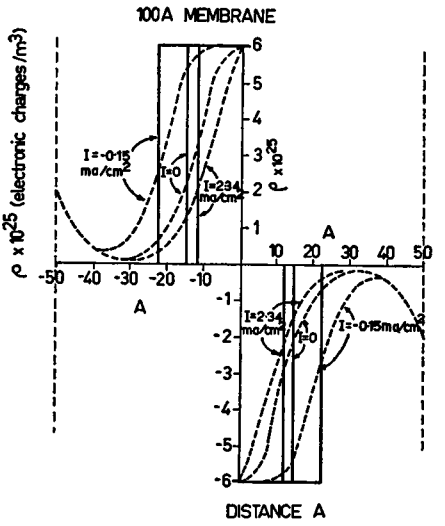

FIGURE 6 Space charge density profiles for a 100 A membrane at a current density of $J = +2.34$ ma/cm² (depolarizing), $J = 0$ and $J = -0.15$ ma/cm² (hyperpolarizing). The full curves are the idealized profiles obtained with the semi-analytic approach and the dashed curves were obtained from the computer analysis. Note that the space charge region in each lattice increases in width on hyperpolarization and decreases on depolarization.

space charge profiles calculated from the SA model are shown for reference (full curves). The effect of current density on the space charge profiles for a 100 A membrane is shown in Fig. 6.

The space charge distributions display several important features. Firstly, strong localized space charge regions do exist at the junction of the two fixed charge lattices and the space charge density, at least close to the center of the membrane, is almost equal to the fixed charge concentration. For regions more removed from the lattice junction, space charge density is small. In this respect the basic ideas of the SA model and Mauro's (1962) analysis are substantiated. However, quantitatively the profiles of space charge show deviations from the idealized model.

Secondly, since the space charge profiles are not the step functions predicted by the SA model, it is impossible to define uniquely the depletion layer boundary. Whatever criterion about space charge density is arbitrarily adopted to define the depletion layer boundary, it is clear from the results in Fig. 6 that the thickness of the depletion layer increases with hyperpolarizing current and decreases with depolarizing current. The profiles of space charge remain almost constant in form as they move in and out with different current densities. In these respects, again the SA model provides qualitatively the correct mechanism.

Thirdly, the assumption of completely uncompensated fixed charge in the depletion layer improves with hyperpolarization. This, however, is coupled with an increase in space charge in the regions outside the depletion layer. In fact for the hyperpolarizing current of -0.15 ma/cm² the profile of space charge outside the depletion layer is not only significant but is also not constant anywhere in this region. The latter is also reflected in the potential profiles (Figs. 3 and 4). The agreement between the computer results and the SA model improves, however, as the total membrane thickness increases.

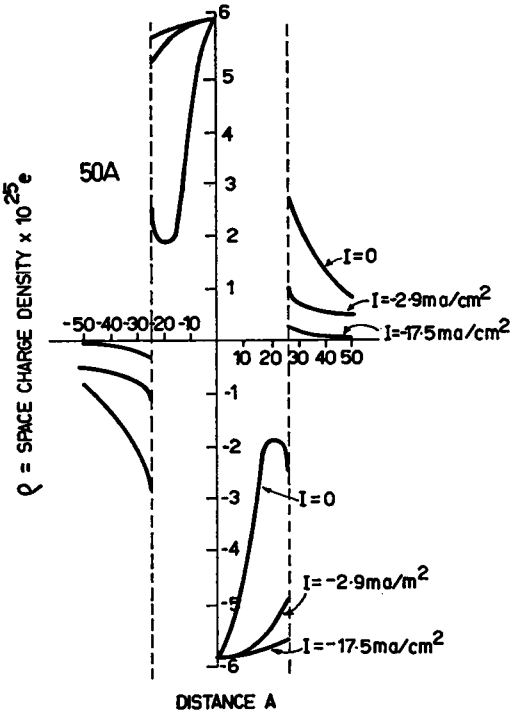

FIGURE 7 Space charge profiles for a 50 A membrane at three current densities (hyperpolarizing), obtained with the computer analysis. With reference to Fig. 2 it can be seen that as the punch-through effect is approached, the space charge region in each lattice extends right through to the membrane boundary. Similar results for thicker membranes could not be obtained owing to limitations in computer accuracy.

Furthermore, when the space charge region of the depletion layer approaches the membrane boundary, the punch-through effect begins to set in. In the idealized model this was a clear-cut process, the end point being an impossible situation, but nevertheless, mathematically well-defined. The results obtained with the computer analysis show that the space charge profiles begin to interfere with the membrane–solution phase boundary (which has its own space charge region) at smaller potentials than that predicted by the SA model. This effect is illustrated in Fig. 7 which shows the space charge profiles for a 50 A membrane at three hyperpolarizing current densities. For the thicker membranes, for which the SA approach appears to be a better approximation, similar results could not be obtained owing to limitations in computer accuracy.

At large hyperpolarizations the space charge region at the membrane boundary interferes with that of the depletion layer. This is accompanied by an increase in the fraction of the total potential drop (PD) which is developed across the membrane-solution boundaries. It appears likely that these effects delay the final punch-through effect in the voltage-current curves (see Fig. 2).

Ion Profiles

The profiles of mobile ion concentration are of considerable interest since they provide a graphic indication of the degree of validity of the assumptions made in the semianalytic analysis.

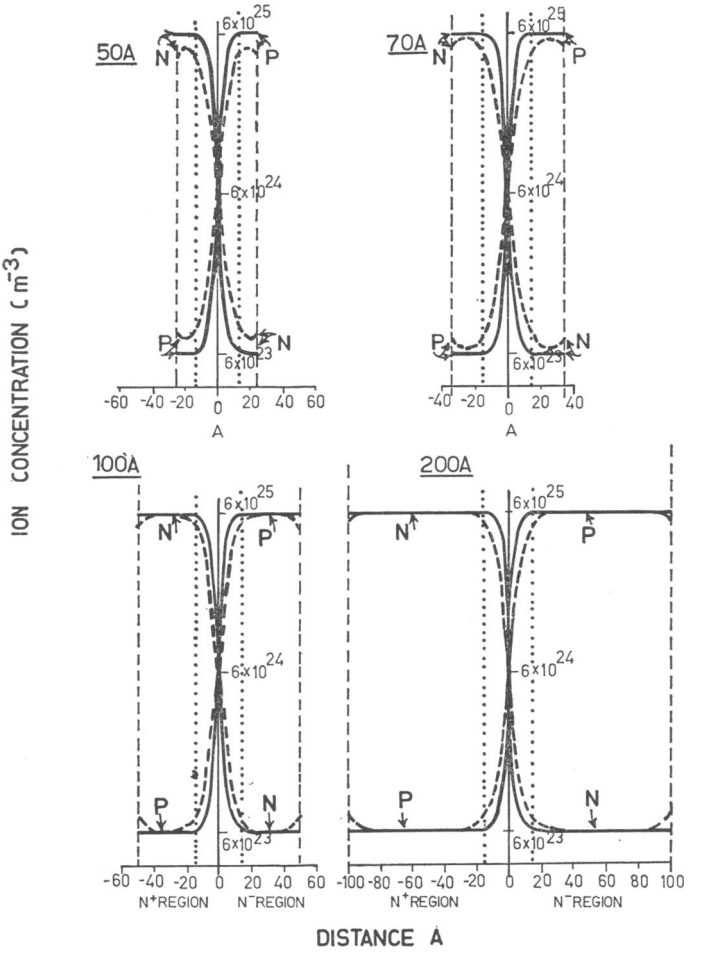

FIGURE 8 Profiles of mobile ion concentration in a 50, 70, 100, and 200 A double fixed charge membrane at zero current density. The negative mobile ions are in the majority in the positive fixed charge lattice (left half) and vice versa. The full curves were obtained from the semianalytic analysis and the broken curves from the computer results. The boundaries of the depletion layer (as calculated from the semianalytic analysis) are indicated by the dotted vertical lines.

Fig. 8 shows the computer results for the ion concentration profiles for a 50, 70, 100, and 200 A membrane when no current is present. The full curves were obtained from the semianalytic approach while the broken curves were obtained from the computer analysis. Note that a logarithmic scale is used for concentration.

Fig. 9 shows the profiles of ion concentration (again on a logarithmic scale) for a 100 A membrane at three current densities. Fig. 10 gives the corresponding profiles for the minority ion concentration on a linear scale.

The essential feature of the ion profiles is that the minority ion concentration outside the depletion layer is several orders of magnitude smaller than the majority ion

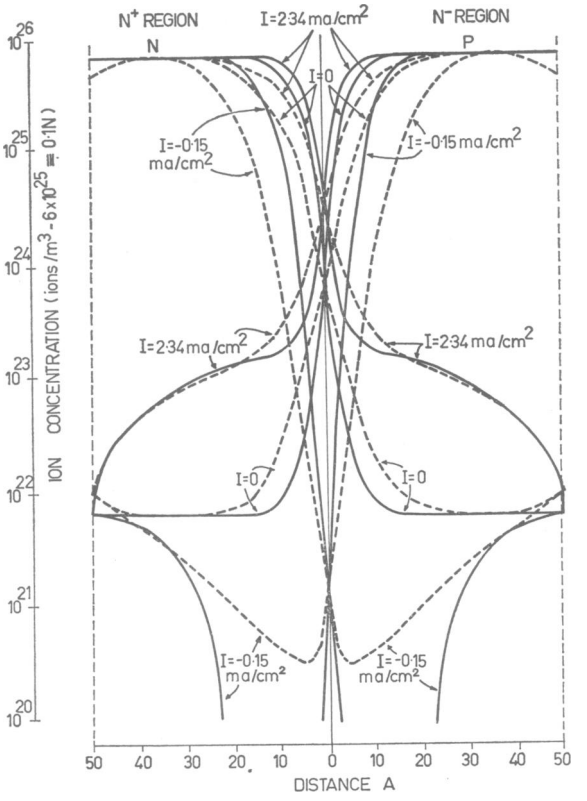

FIGURE 9 Ion concentration profiles, on a logarithmic scale, for a 100 A membrane at a current density $J = +2.34$ ma/cm² (depolarizing) $J = 0$ and $J = -0.15$ ma/cm² (hyperpolarizing). The full curves were obtained from the semianalytic approach and the broken curves from the computer analysis.

concentration, the latter having a concentration almost equal to that of the fixed charge concentration.

The analysis of Coster assumes a flat profile for the ion concentrations in the membrane, outside the depletion layer, when no current is flowing. In that analysis this should still be true for the majority ions when a current is present. It can be seen from Figs. 8 and 9 that the computer results do not justify this assumption for the thinner membranes. For the thicker membranes, however, this assumption seems to be confirmed by the computer results.

The linear gradient of the minority ion concentration, which follows from the SA approach when a current is present, is in good agreement over a substantial region for depolarizing currents. The agreement in fact, improves as the depolarizing current increases (not shown in diagram). For large hyperpolarizing currents the agreement is not so good.

It should be noted that the minority ion concentration at the depletion layer

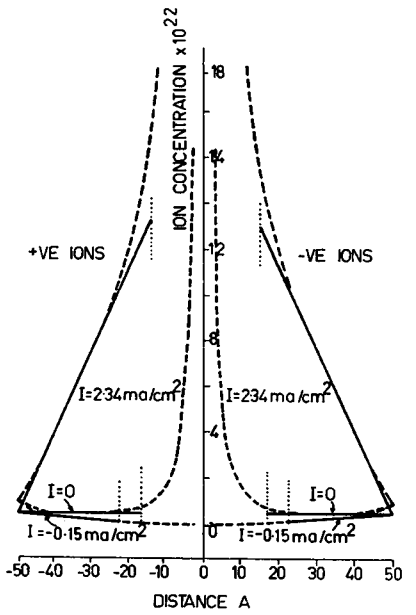

FIGURE 10 Profiles of minority ion concentration for a 100 A membrane, on a linear scale, at the same current densities as in Fig. 9. The depletion layer boundary is indicated in each case by the dotted vertical lines. For the hyperpolarizing current of -0.15 ma/cm², the minority ion concentration at the depletion layer boundary is essentially zero.

boundary predicted by the SA approach, tends to be underestimated by a large factor. The relative discrepancy increases with hyperpolarization. However, the absolute error in this minority ion concentration at the depletion layer boundary is very small since even for moderate hyperpolarizations (-100 mv) this value is essentially equal to zero. Hence, the error in the gradient of the minority ion concentration is small even for large hyperpolarizing currents.

The Boltzmann Distribution

Another fundamental assumption made in the semianalytic approach, is that the minority ion concentration at the depletion layer boundary, can be obtained from the concentration of the same ions in the opposite fixed charge lattice, using the Boltzmann distribution function. It is thus assumed that long-range equilibrium exists across the depletion layer even when currents are present (some justification of this assumption can be given—see Discussion). Outside the depletion layer the minority ions are not in equilibrium when a current is present.

The validity of the use of Boltzmann statistics across the depletion layer could be tested by comparison with the numerical computer analysis.

As might be expected, it was found that generally the Boltzmann distribution ratio did not agree with the computer values. The deviation from the Boltzmann distribution ratio was a function of the current density and was much more serious with hyperpolarizing currents, where this ratio is much too large, than with depolarizing currents, where it is too small.

TABLE I

COMPARISON OF THE ION DISTRIBUTION RATIO FOR A 100 A MEMBRANE

Current density	Ion distribution ratio		
	Computer analysis	SA model	Boltzmann using computer profile for ψ
+2.34 ma/cm² (depolarizing)	2×10^{3}	4×10^{3}	1.5×10^{3}
0	0.66×10^{4}	1.0×10^{4}	0.66×10^{4}
−0.15 ma/cm² (hyperpolarizing)	3.0×10^{4}	1.0×10^{10}	6×10^{8}

In the SA analysis, however, the electrostatic potential difference, across the depletion layer, is higher than the actual values (see Figs. 8 and 9). The Boltzmann distribution ratio derived from electrostatic potential differences obtained from the computer analysis is therefore not identical to those derived from the SA model.

Table I gives a comparison of the ion distribution ratio across the depletion layer for a 100 A membrane, for the computer results, the semianalytical approach, and Boltzmann statistics using computer PD's, at three current densities.

Membrane Capacitance

The width of the space charge regions in the depletion layer are functions of the current density (and hence applied potential). Using the idealized profiles, like those shown in Figs. 5 and 6, Mauro (1962) derived an expression for the differential capacitance of the junction at zero applied bias.

This treatment can be readily extended to obtain the differential capacitance as a function of applied bias, using the variation of the depletion layer width with potential predicted by the SA model. The differential capacitance determined from the total stored charge as a function of applied potential, was also obtained from the computer analysis.

Fig. 11 shows the results for the differential capacitance using both methods of analysis, for a 100 A membrane. For thick membranes the differential capacitance at zero applied bias, determined from the computer analysis, is independent of membrane thickness and has a value of about 3.4 $\mu F/cm^2$. At zero applied potential the SA model (full curve) tends to underestimate the capacitance.

At large hyperpolarizations the differential capacitance decreases more rapidly than that predicted by the SA model. This is due to the fact that the depletion-layer space charge profiles are interfering with those near the membrane boundaries. The total change in space charge with applied potential is consequently less than that predicted by the SA approach.

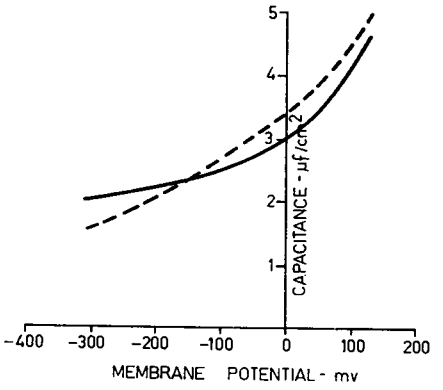

FIGURE 11 The differential capacitance for a 100 A double fixed charge membrane as a function of the applied bias. The full curve was obtained by extending the expression derived by Mauro (1962), using the dependence of the depletion layer thickness on the applied bias given by the semianalytic approach. The dashed curve was obtained from the computer analysis.

DISCUSSION

Comparison of the various parameters obtained from the semianalytic analysis and the computer results show that quantitative agreement is achieved over a good range of current densities and membrane thicknesses.

The numerical analysis with the computer is very time consuming. A single run can take up to 30 min or even more at small current densities, and increases with the current density especially in the hyperpolarizing region. The investigation of the effects of various parameters such as ion concentration, dielectric constant, ion mobility, fixed charge concentration, etc. could thus become a prohibitively costly task. Furthermore, the present method of numerical analysis becomes even more involved when a nonsymmetrical system is used.

Since the semianalytic analysis lends itself much more readily to such investigations it is of importance to have a guide to determine its range of validity.

Ion Profiles

One of the main assumptions made in the SA approach is that the ion profiles level out in the membrane, outside the depletion layer. It is apparent that this can only be justified for membranes whose thickness is 100 A, while for a 50 A membrane this assumption breaks down. The approximation of the idealized to the actual profiles improves with increasing membrane thickness. Furthermore, as the membrane thickness increases from 50 to 100 A the depletion layer becomes much more sharply defined (see Fig. 5), thus enhancing the improvement of the approximation of the ion profiles given by the SA model.

The reverse effect, when the membrane thickness is decreased, eventually gives profiles similar to those published originally by George and Simons (1966) in which the membrane, even at zero current density, is approaching the punch-through condition in which the space charge regions extend throughout the membrane.

Distribution of Applied Potential

The depletion layer has a low total ion concentration, compared with the regions of the membrane outside the depletion layer. This general result, predicted from the SA approach has been confirmed by the computer analysis, although the boundaries of the depletion layer are ill defined.

From this result it was argued that any applied potential appearing across the membrane would appear almost completely across the depletion layer since this has a relatively low conductivity. It was also tacitly assumed that no PD due to currents would appear in the solution phase. For membranes of sufficient thickness ($>\sim$ 70 A) this latter assumption is justified over the range of current densities investigated. The mobility of the ions in the membrane was taken as 10^{-3} of those in the outside solution. The total concentration of mobile ions in the membrane does not exceed the fixed charge concentration, i.e., 100 times the external ion concentration. Thus, the conductivity of the external solution exceeds that of the membrane and the assumption that only small PD's appear in the external solution due to applied currents, appears to be justified. With very large hyperpolarizing currents, however, a sizeable proportion of the potential drop, due to the applied current, takes place across the space charge regions at the solution-membrane boundary. This tends to increase the hyperpolarizing potential at which the final rapid rise in the current sets in as the punch-through region is reached.

The Validity of Boltzmann Statistics

The Boltzmann distribution function is of course not strictly applicable when a current is present.

The current density is given by equations 1. Rearrangement of these equations gives:

$$\frac{dP}{P} = \frac{-Jp}{kT\mu_p}\frac{dx}{p} - \frac{q}{kT}d\psi$$

and

$$\frac{dN}{N} = \frac{Jn}{kT\mu_N}\frac{dx}{N} + \frac{q}{kT}d\psi. \tag{10}$$

It is at once obvious that when $J_n = J_p = 0$, integration of equation 10 yields the Maxwell-Boltzmann distribution function. Furthermore, when the first term on the right-hand side of equation 10 is small compared to the second term, the Boltzmann distribution function will still be approximately valid. That is, as long as

$$\int \frac{Jn}{\mu_n N}dx \ll q\psi, \tag{11}$$

Boltzmann statistics may be used.

For depolarizing currents and small hyperpolarizing currents, J_p and J_n in the depletion layer are small compared to the field current $q\mu_p \, d\psi/dx$ or the concentration current $kT\mu_p \, dP/dx$. The contrary is true for the minority ions in the regions of the membrane outside the depletion layer. Thus, there is some justification for assuming that equilibrium is approximately maintained across the depletion layer but not for the minority ions in the regions outside this layer. For larger hyperpolarizing currents the Boltzmann distribution function no longer predicts the correct minority ion concentration at the depletion layer boundary. However, at large hyperpolarizing currents the error introduced is inconsequential since the concentration of minority ions at the depletion layer boundary is essentially zero (see Ion Profiles in Results).

Voltage-Current Characteristics

These tend to be predicted correctly by the semianalytic analysis over a wider range than might be expected from the profiles of various parameters such as ion concentration, etc.

The current density predicted from the SA model is obtained from the gradient of minority ions, there being no contribution from a minority ion field current. The current carried by majority ions of the same sign in the opposite fixed charge lattice is of equal magnitude and thus maintains the minority ion profile.

When the idealized profiles of the SA model are not manifested in any substantial portion of the membrane, e.g., for a 50 A at an applied bias of -300 mv, the correct current density can still result, provided that the minority ion gradient is equal to the actual gradient at some point or region where the electric field is very small. The gradient of minority ions for hyperpolarizing currents, predicted by the SA model, is not greatly in error despite the gross shortcomings in determining the concentration at the depletion-layer boundary. This occurs because the latter value is essentially zero relative to the absolute value of the concentration of minority ions near the solution-membrane boundary. The latter is also reflected in the voltage-current curves (Fig. 2) which show that for moderate hyperpolarizing potentials the current density is essentially constant.

CONCLUSIONS

The physical processes responsible for the electrical characteristics predicted by the semianalytic analysis have been verified by the computer results. There are, however, some quantitative differences. The results presented allow us to conclude that:

1. Voltage-current characteristics for membranes $\geqq 70$ A are correctly predicted by the semianalytic analysis over the range of potentials -700 to $+100$ mv (-0.7 to $+$ 5.0 ma/cm^2). For the 50 A membrane, quantitative ($>10\%$)

differences in current densities begin at -200 mv, although for more positive potentials the fit is good.

2. Profiles of electrostatic potential and ion concentrations are good approximations for membranes > 100 A in thickness, but gradually deteriorate until for a 50 A membrane they are seriously in error.

3. Space charge profiles never approach the idealized step functions of the SA analysis, although for thick membranes they are highly localized. The widths of these space charge regions vary with applied potential in a similar manner to that predicted.

4. The punch-through effect which results from the dependence of the dimensions of the depletion layer on the applied potential, has been verified qualitatively. The semianalytic analysis tends to underestimate the punch-through potential.

5. The correctness of the semianalytic analysis improves with depolarization and with increasing membrane thickness (and vice versa).

6. In general for all currents removed from the punch-through region the semianalytic analysis gives a good fit.

7. The capacitance of the membrane is given to a good approximation by the analysis of Mauro (1962). Qualitatively, the dependence of the capacitance on applied potential predicted by the SA model has been verified, although at large hyperpolarizations the capacitance decreases more rapidly than that predicted by the SA analysis.

8. When currents are present ionic concentrations obtained from the computer results do not agree with those predicted from the Boltzmann distribution function. The disagreement is not very serious for depolarizing currents but deteriorates progressively with increasing hyperpolarizing currents.

Received for publication 4 November 1968.

REFERENCES

CONTI, F., and G. EISENMAN. 1965 *a*. *Biophys. J.* **5**:247.
CONTI, F., and G. EISENMAN. 1965 *b*. *Biophys. J.* **5**:511.
COSTER, H. G. L. 1965. *Biophys. J.* **5**:669.
COSTER, H. G. L. 1969. *Aust. J. Biol. Sci.* **22**:365.
COSTER, H. G. L., and A. B. HOPE. 1968. *Aust. J. Biol. Sci.* **21**:243.
EISENMAN, G. 1960. Symposium on Membrane Transport and Metabolism. Academic Press Inc., New York. 163.
EISENMAN, G. 1962. *Biophys. J.* **2** (Suppl. 2):259.
GEORGE, E. P., and R. SIMONS. 1966. *Aust. J. Biol. Sci.* **19**:459.
KARREMAN, G., and G. EISENMAN. 1962. *Bull. Math. Biophys.* **24**:413.
MAURO, A. 1962. *Biophys. J.* **2**:179.
MEYERS, K. H., and J. F. SIEVERS. 1936. *Helv. Chim. Act.* **19**:649.
TEORELL, T. 1953. *Progr. Biophys. Biophys. Chem.* **3**:30.
WILLIAMS, E. J., and J. BRADLEY. 1968. *Biophys. J.* **8**:145.